AMERICAN ACADEMY OF OPHTHALMOLOGY®

X-Linked Retinoschisis

Novel Clinical Observations and Genetic Spectrum in 340 Patients

Leo C. Hahn, MD,[1] Mary J. van Schooneveld, MD, PhD,[1,2] Nieneke L. Wesseling, MD,[1] Ralph J. Florijn, PhD,[3] Jacoline B. ten Brink, BAS,[3] Birgit I. Lissenberg-Witte, PhD,[4] Ine Strubbe, MD,[5] Magda A. Meester-Smoor, PhD,[6] Alberta A. Thiadens, MD, PhD,[6] Roselie M. Diederen, MD, PhD,[1] Caroline van Cauwenbergh, PhD,[5,7] Julie de Zaeytijd, MD,[5] Sophie Walraedt, MD,[5] Elfride de Baere, MD, PhD,[5,7] Caroline C.W. Klaver, MD, PhD,[6,8,9] Jeannette Ossewaarde-van Norel, MD, PhD,[10] L. Ingeborgh van den Born, MD, PhD,[11] Carel B. Hoyng, MD, PhD,[8] Maria M. van Genderen, MD, PhD,[2,10] Paul A. Sieving, MD, PhD,[12] Bart P. Leroy, MD, PhD,[5,13] Arthur A. Bergen, PhD,[3,14] Camiel J.F. Boon, MD, PhD[1,15]

Purpose: To describe the natural course, phenotype, and genotype of patients with X-linked retinoschisis (XLRS).

Design: Retrospective cohort study.

Participants: Three hundred forty patients with XLRS from 178 presumably unrelated families.

Methods: This multicenter, retrospective cohort study reviewed medical records of patients with XLRS for medical history, symptoms, visual acuity (VA), ophthalmoscopy, full-field electroretinography, and retinal imaging (fundus photography, spectral-domain [SD] OCT, fundus autofluorescence).

Main Outcome Measures: Age at onset, age at diagnosis, severity of visual impairment, annual visual decline, and electroretinography and imaging findings.

Results: Three hundred forty patients were included with a mean follow-up time of 13.2 years (range, 0.1−50.1 years). The median ages to reach mild visual impairment and low vision were 12 and 25 years, respectively. Severe visual impairment and blindness were observed predominantly in patients older than 40 years, with a predicted prevalence of 35% and 25%, respectively, at 60 years of age. The VA increased slightly during the first 2 decades of life and subsequently transitioned into an average annual decline of 0.44% ($P < 0.001$). No significant difference was found in decline of VA between variants that were predicted to be severe and mild ($P = 0.239$). The integrity of the ellipsoid zone (EZ) as well as the photoreceptor outer segment (PROS) length in the fovea on SD OCT correlated significantly with VA (Spearman's $\rho = -0.759$ [$P < 0.001$] and -0.592 [$P = 0.012$], respectively). Fifty-three different *RS1* variants were found. The most common variants were the founder variant c.214G→A (p.(Glu72Lys)) (101 patients [38.7%]) and a deletion of exon 3 (38 patients [14.6%]).

Conclusions: Large variabilities in phenotype and natural course of XLRS were seen in this study. In most patients, XLRS showed a slow deterioration starting in the second decade of life, suggesting an optimal window of opportunity for treatment within the first 3 decades of life. The integrity of EZ as well as the PROS length on SD OCT may be important in choosing optimal candidates for treatment and as potential structural end points in future therapeutic studies. No clear genotype−phenotype correlation was found. *Ophthalmology 2022;129:191-202*

Supplemental material available at www.aaojournal.org.

X-linked retinoschisis (XLRS) is among the most common degenerative retinopathies. It is estimated to develop in approximately 1 in 5000 to 1 in 20 000 boys and young men worldwide, which is comparable with the prevalence of Stargardt disease.[1] The phenotype of XLRS was documented in 1889 by the ophthalmologist Haas, but various names were used to describe this disease in 1953, when Jager coined the term X-linked retinoschisis.[2,3] Patients typically demonstrate mild to moderate, bilateral, nonacutely reduced central vision within the first 2 decades of life and splitting of retinal layers in the macula. X-linked retinoschisis may also present as a congenital condition in some patients, because severe retinoschisis in the macula or peripheral retina has been described in patients as young as

https://doi.org/10.1016/j.ophtha.2021.09.021
ISSN 0161-6420/21

3 months of age.[1,4] Many patients with XLRS typically have central radial streaks resulting from macular retinoschisis (spoke-wheel pattern) on funduscopy, and peripheral retinoschisis occurs in approximately 50% of patients. Common findings on full-field electroretinography are a reduced b-to-a amplitude ratio, or even an electronegative electroretinography.[5,6] Most patients demonstrate visual acuity (VA) of 20/60 to 20/120 at the first visit. Nonetheless, the phenotype and natural course may be highly variable even within families, ranging from patients with near-normal vision to blindness.[1,6] Although VA may remain relatively stable in XLRS for years, an acceleration of vision loss resulting from central retinal atrophy in the fourth to fifth decades of life has been described.[1,7,8] In addition, patients with XLRS have an increased risk of developing vision-threatening complications such as retinal detachment, vitreous hemorrhages, and neovascular glaucoma.[6]

X-linked retinoschisis is caused by mutations in the *RS1* gene and affects only males because of an X-linked recessive inheritance pattern. Female carriers are generally asymptomatic, but can display minor changes on multifocal electroretinography.[1,9] Some very rare symptomatic female carriers with typical XLRS phenotype have been described, but they either harbored homozygous *RS1* variants or were thought to have skewed X-inactivation.[10,11] The *RS1* gene (Online Mendelian Inheritance in Man identifier, * 300839) encodes a 224-amino acid protein called retinoschisin, which is expressed in bipolar and photoreceptor cells.[1,12] It is secreted into the extracellular space, where it is thought to play an essential role in cell-to-cell adhesion and signal transduction between photoreceptors and bipolar cells.[1,13] Retinoschisin forms a double-octamer structure, coupling neighboring cell membranes through octamer−octamer contact, but the exact molecular mechanism has not been unraveled yet. To date, more than 200 different disease-causing variants of *RS1* have been described. The most common *RS1* variant types are missense variants, most of which are thought to result in intracellular retention and degradation of retinoschisin.[14] No genotype−phenotype correlations have been firmly established thus far, which may be because of relatively small sample sizes of individual studies and variability in phenotype even within families.[15,16]

No proven effective treatment for XLRS is available to date. Carbonic anhydrase inhibitors have been shown to reduce schisis cavities in some patients with XLRS, but no convincing long-term effect on visual function has been established yet.[5,17,18] Experimental intravitreal gene therapy with adeno-associated viruses resulted in anatomic improvement on OCT and functional improvement on electroretinography in knockout mouse models for XLRS.[19,20] Two human intravitreal adeno-associated virus-based gene therapy trials did not show similar improvements, although treatment was well tolerated in these small cohorts.[21] Still, as a monogenetic and a relatively common and severe retinal dystrophy, XLRS remains an attractive target for (gene) therapeutic intervention. Because gene therapeutic possibilities are advancing rapidly, a thorough understanding of clinical features, variability in phenotype, and long-term natural history of inherited retinopathies such as XLRS is crucial for selecting optimal eligibility criteria and end points for future gene therapy trials. We assembled one of the largest XLRS cohorts to date with the aim of describing a detailed phenotypic spectrum, the long-term development of clinical characteristics, and potential genotype−phenotype correlations.

Methods

Study Population

Patients with XLRS as a clinical diagnosis and at least 1 recorded clinical visit were identified for this study. To be included, XLRS had to be confirmed molecularly as a pathogenic variant in the *RS1* gene in the index patient or a family member. After thorough examination of the medical records, inclusion was possible in the case of an evident X-linked inheritance pattern over multiple generations, in combination with a typical and unambiguous clinical presentation of XLRS. Eyes were excluded from further analysis when visual function was lost because of factors other than the natural XLRS disease process, such as trauma. Of the 352 eligible patients who were identified, 12 had to be excluded because of ocular trauma, ambiguous information regarding their diagnosis, or insufficient clinical data. Additionally, 3 eyes were excluded from the analyses for the following reasons: a retrobulbar abscess requiring surgery, perforating trauma, and vision loss resulting from toxoplasma chorioretinitis. Patient data were gathered from the Delleman archive, a large database for hereditary eye diseases of the Amsterdam University Medical Centers (Amsterdam, The Netherlands), and from various Dutch centers within the RD5000 consortium, a nationwide collaborative registry for patients with retinal dystrophies.[22] Additionally, data from the Ophthalmic Genetics Unit at the Department of Ophthalmology & Center for Medical Genetics Ghent (Ghent, Belgium) were included. This study was approved by the Medical Ethics Committee of the Amsterdam University Medical Centers, Erasmus Medical Center, and Ghent University Hospital. It adhered to the tenets of the Declaration of Helsinki, and informed consent was obtained from patients or their legal guardians. The need for informed consent was waived by the local ethics committee of the University Hospital Ghent because of the use of pseudonymized data.

Clinical Data Collection

Data were collected by extensively reviewing all medical records for medical history, age at onset, symptoms, age at diagnosis, XLRS-associated complications, familial history, VA, refractive error, dilated fundus examination findings, full-field electroretinography findings, spectral-domain (SD) OCT images, fundus autofluorescence images, and color fundus photography, if available. For 261 patients, the specific variant in the *RS1* gene could be collected or derived from a family member. These variants have been confirmed molecularly through Sanger sequencing or whole-exome sequencing. The age at onset was defined as the year in which the first symptoms associated to XLRS were noted. If amblyopia was mentioned in the records, it was confirmed by checking for a difference in VA of at least 2 lines (0.3 logarithm of the minimum angle of resolution [logMAR]) between both eyes at multiple visits). Additionally, factors other than amblyopia that could have caused asymmetry between eyes were ruled out. Most SD OCT scans were obtained using a Heidelberg Spectralis (Heidelberg Engineering, Heidelberg, Germany). Some centers used a Topcon (3D OCT-1000; Topcon Medical Systems) or Canon OCT-

HS100 (Angio eXpert, OCTA version 2.0; Canon). The following retinal parameters were assessed on SD OCT: central retinal thickness, foveal volume, photoreceptor outer segment (PROS) length, and the integrity of the external limiting membrane (ELM) as well as the ellipsoid zone (EZ) within a 1000-μm central subfield area, based on 3 categories: intact, disrupted, and absent. The PROS length was defined as the foveal distance between the inner EZ layer and the inner surface of the retinal pigment epithelium (RPE). Electroretinography examination results were categorized based on reports as within normal range, reduced b-to-a amplitude ratio in case of a significantly reduced b-wave amplitude, or as electronegative if the b-wave amplitude was smaller than the a-wave amplitude on scotopic electroretinography obtained with a high-intensity flash stimulus (3 or 10 cd·s/m^2). For patients who received carbonic anhydrase inhibitor treatment, SD OCT images and electroretinography examination after the initial dose were not included in the analysis.

Statistical Analysis

All analyses were performed in SPSS software version 25.0 (IBM Corp), except for the linear mixed-effects models and the time-to-event analysis, which was carried out in R software version 3.3.1 (R Foundation for Statistical Computing). Categorical data were expressed as proportions. Continuous data were expressed as either means with standard deviations or medians with interquartile ranges (IQRs). Time-to-event analysis was performed to estimate the age to reach the following states of visual impairment according to the World Health Organization: mild visual impairment (VA, <20/40 and ≥20/70), low vision (VA, <20/70 and ≥20/200), severe visual impairment (VA, <20/200 and ≥20/400), and blindness (VA, <20/400). For this analysis, the nonparametric maximum likelihood estimator method was used to account for left-censored, interval-censored, and right-censored data. To determine the annual decline rate of VA, the VA was converted to logMAR values, with 2.7 logMAR used for hand movements, 2.8 logMAR used for light perception, and 2.9 logMAR used for no light perception. Subsequently, the annual decline rate in logMAR was estimated using the VA of the right eye in a linear mixed-effects model, which was corrected for carbonic anhydrase inhibitor use. The same model was used to determine genotype−phenotype correlations. For calculating genotype−phenotype correlations, variants were classified as mild (missense variant) or severe (deletions, nonsense, splice site, frameshift, and cysteine substitutions-causing variants) as described earlier.[23] Because VA in children is still developing and only reaches adult-like vision in the beginning of the second decade, and decline of VA may accelerate with increasing age because of the development of atrophy, splines were calculated to check for a better-fitting model.[24,25] The right eye was selected randomly to be used for analyses of VA and visual impairment to prevent biases associated with between-eye correlation, which is present in analyses using both or the better-seeing eye.[26]

Results

A total of 340 patients from 178 presumably unrelated families were included. For 173 patients, a disease-causing variant in the *RS1* gene was confirmed molecularly. Another 88 patients had received a clinical diagnosis of typical XLRS and had a first- or second-degree family member with a confirmed disease-causing variant in the *RS1* gene. For the remaining 79 patients, no genetic testing was available. These patients were included based on an unambiguous clinical diagnosis of XLRS, presence of bilateral macular spoke-wheel pattern, a reduced b-to-a amplitude ratio, and an X-linked inheritance pattern within the family. Four patients were reported previously, but additional follow-up data have become available for this study.[17] For 273 patients, follow-up data were available with a mean follow-up time of 13.2 ± 11.8 years (range, 0.1−50.1 years). The mean number of visits per patient was 6.8 ± 8.0 visits (range, 1.0−57.0 visits; Table 1). The distribution of the number of visits and follow-up time among included patients is specified in Table S2 (available at www.aaojournal.org).

Clinical Presentation and Visual Function

The age at onset and age at diagnosis were reported for 177 patients. The median age at onset was 4.0 years (IQR, 1.0−6.0 years; range, 0.0−39.0 years), and the median age at diagnosis was 7.0 years (IQR, 4.0−19.0 years; range, 0.0−70.0 years).

Bilateral VA data were available for 328 of 340 patients. The median VA at last examination was 0.60 logMAR (IQR, 0.40−0.92 logMAR; median, 20/80 Snellen equivalent; IQR, 20/166−20/50 Snellen equivalent) for the right eye and 0.53 logMAR (IQR, 0.40−0.82 logMAR; median, 20/68 Snellen equivalent; IQR, 20/132−20/50 Snellen equivalent; Table 1) for the left eye. The survival curves for visual impairment and the linear mixed model predicting longitudinal evolution of VA are presented in Figure 1. The median ages to reach mild impairment and low vision were 12 years and 25 years, respectively. Because of insufficient events, the median age to reach severe visual impairment or blindness could not be calculated, but for both, a similar slowly increasing occurrence was seen from the first to fourth decade of life in less than 15% of patients. At approximately the fifth decade of life, an acceleration of this trend was seen, and at the age of 60 years, approximately 35% and 25% of patients were predicted to have reached severe visual impairment and blindness, respectively. The mean annual decline rate of VA in the right eye was 0.44% ($P < 0.001$), and no significant difference was seen in the visual decline rate between variants that were predicted to be mild or severe ($P = 0.239$). Repeating these analyses for the left eye yielded similar results with an annual decline rate of 0.38% ($P < 0.001$), and also no significant genotype−phenotype correlation ($P = 0.644$).

A moderate symmetry between the VA of the right and left eyes was seen (Spearman's $\rho = 0.541$; $P < 0.001$). A total of 97 of 273 patients (35.5%) showed an asymmetry in VA of at least 0.3 logMAR between the left and right eyes for at least 2 consecutive visits.

Clinical Findings in X-Linked Retinoschisis

The mean spherical equivalent refractive error was +2.0 ± 2.7 diopters (D; range, −7.2 to +9.6 D), with a mean astigmatism of −1.2 ± 1.1 D. In 240 of 334 patients (70.4%), cystic changes in the macula were reported on funduscopy, and spoke-wheel pattern was reported in 173 of 334 patients (50.7%). Macular atrophy was described in 30 of 335 patients (8.8%), who had a mean age of 36.4 ± 22.3

Table 1. Clinical Characteristics of X-linked Retinoschisis Patients

Characteristics	Data XLRS patients (n = 340)
Age at last examination (yrs)	
Mean ± SD	28.6±19.3
Median (IQR)	21.9 (Q1: 13.2, Q3: 43.4)
Range	0.4–85.6
No. of visits	
Mean ± SD	6.8±8.0
Median (IQR)	4.0 (Q1: 2.0, Q3: 10.0)
Range	1.0–57.0
Follow-up time (n = 273, yrs)	
Mean ± SD	13.2±11.8
Median (IQR)	10.1 (Q1: 4.3, Q3: 18.2)
Range	0.1–50.1
Age at onset (n = 177)	
Median (IQR)	4.0 (Q1: 1.0, Q3: 6.0)
Range	0.0–39.0
Age at diagnosis (n = 177)	
Median (IQR)	7.0 (Q1: 4.0, Q3: 19.0)
Range	0.0–70.0
Spherical equivalent refractive error, D (n = 198)	
Mean ± SD	2.0±2.7
Range	-7.2 to 9.6
Last available VA in the right eye (n = 328)	
Median VA, in logMAR (IQR)	0.60 (Q1: 0.40, Q3: 0.92)
Median VA, in Snellen equivalent (IQR)	20/80 (Q1: 20/166, Q3: 20/50)
Last available VA in the left eye (n = 328)	
Median VA, in logMAR (IQR)	0.53 (Q1: 0.40, Q3: 0.82)
Median VA, in Snellen equivalent (IQR)	20/68 (Q1: 20/132, Q3: 20/50)
Nystagmus, no./total (%)	20/340 (5.9%)
Strabismus, no./total (%)	60/340 (17.6%)
Amblyopia no./total (%)	22/340 (6.5%)
Funduscopic examination, no./total (%)*	
Macular retinoschisis	240/334 (70.4%)
Spoke-wheel pattern	173/334 (50.7%)
Macular RPE atrophy	30/335 (8.8%)
Macular RPE alterations	90/334 (26.4%)
Optic disk pallor	54/338 (15.8%)
Peripheral retinoschisis	177/337 (51.9%)
Vitreous veils	41/338 (12.0%)
Full-field electroretinogram pattern, no./total (%)	
Normal, no./total (%)	2/54 (3.7%)
Reduced b-to-a amplitude ratio, no./total (%)	13/54 (24.1%)
Electronegative	39/54 (72.2%)

VA = visual acuity; D = diopters; IQR = interquartile range; logMAR = logarithm of the minimum angle of resolution; RPE = retinal pigment epithelium; SD = standard deviation; XLRS = X-linked retinoschisis.
*Patients could present multiple different fundoscopic abnormalities simultaneously.

years (range, 3.25–71.4 years) at first recorded report. Peripheral retinoschisis was described in 177 of 337 patients (51.9%), and optic disc pallor was reported in 54 of 334 patients (15.8%). The most common findings described above are displayed in Figure 2. The following more atypical findings were reported: Coats-like lesions were found in 4 of 340 patients (1.2%), a retinitis pigmentosa-like aspect was found in 3 of 340 patients (0.9%), chorioretinal scars were found in 6 of 340 patients (1.8%), and fundus albipunctatus-like depositions were found in 2 of 340 patients (0.6%; Fig 3).

In total, 45 of 340 patients (13.2%) demonstrated vitreous hemorrhage at a median age of 9.4 years (IQR, 5.7–20.3 years; range, 0.5–62.6 years). Retinal detachment was described in 29 patients (8.5%) and was reported at a median age of 9.0 years (IQR, 2.8–17.7 years; range, 0.6–61.6 years). Glaucoma was found in 13 patients (3.8%) at a mean age of 11.0 years (IQR, 7.6–17.9 years; range, 1.9–38.6 years). One patient (0.3%) was reported with a falciform retinal detachment (Fig 3C). Cataract was present in 17 patients (5%), of whom 10 underwent uncomplicated cataract surgery at a median age of 36.0 years (IQR, 10.1–48.6 years; range, 1.6–71.3 years) during follow-up. A total of 56 of 340 patients (16.5%) received treatment with carbonic anhydrase inhibitors at some point.

Full-Field Electroretinography and OCT

Full-field electroretinography data were available for 54 patients at a median age of 14.1 years (IQR, 7.1–41.8 years; range, 0.3–63.8 years). Only 2 of 54 patients (3.7%) showed a normal electroretinography pattern at an age of 3 and 6 years. Thirteen patients (24.1%) showed a reduced b-to-a amplitude ratio, and 39 patients (72.2%) showed an electronegative electroretinography pattern (Table 1).

Spectral-domain OCT imaging was analyzed in 120 eyes at a median age of 18.6 years (IQR, 12.1–27.4 years; range, 3.9–69.3 years) at examination (Table S3, available at www.aaojournal.org). The mean central retinal thickness was 395.4 ± 219.6 μm, and the mean foveal volume was 0.30 ± 0.14 mm^3 with a high degree of symmetry between eyes (Spearman's $\rho = 0.790$ [$P < 0.001$] and 0.799 [$P < 0.001$], respectively). The mean PROS length was 24.2 ± 9.2 μm and was correlated significantly with VA (Spearman's $\rho = -0.592$; $P < 0.012$). For the integrity of the ELM, a fair to moderate symmetry was seen between eyes (Spearman's $\rho = 0.572$; $P < 0.001$) and for the integrity of the EZ, a high degree of symmetry was found (Spearman's $\rho = 0.795$; $P < 0.001$). The integrity of ELM and EZ both were correlated significantly with VA (Spearman's $\rho = -0.604$ [$P < 0.001$] and -0.759 [$P < 0.001$], respectively).

Genetic Characteristics

In total, the specific variant in the *RS1* gene could be collected or derived from a family member in 261 patients. Of the 53 different disease-causing *RS1* variants found in this cohort, 34 were missense variants, 9 were deletions, 4 were nonsense variants, 2 were splice-site variants, and 1 was a frameshift variant. Most variants were localized in the discoidin domain encoding exons 3, 4, 5, and 6. The location of the reported variants in the *RS1* gene and the retinoschisin protein are displayed in Figure 4. The most common variants were the founder variant c.214G→A (p.(Glu72Lys); 101 patients [38.7%]), a deletion of exon 3

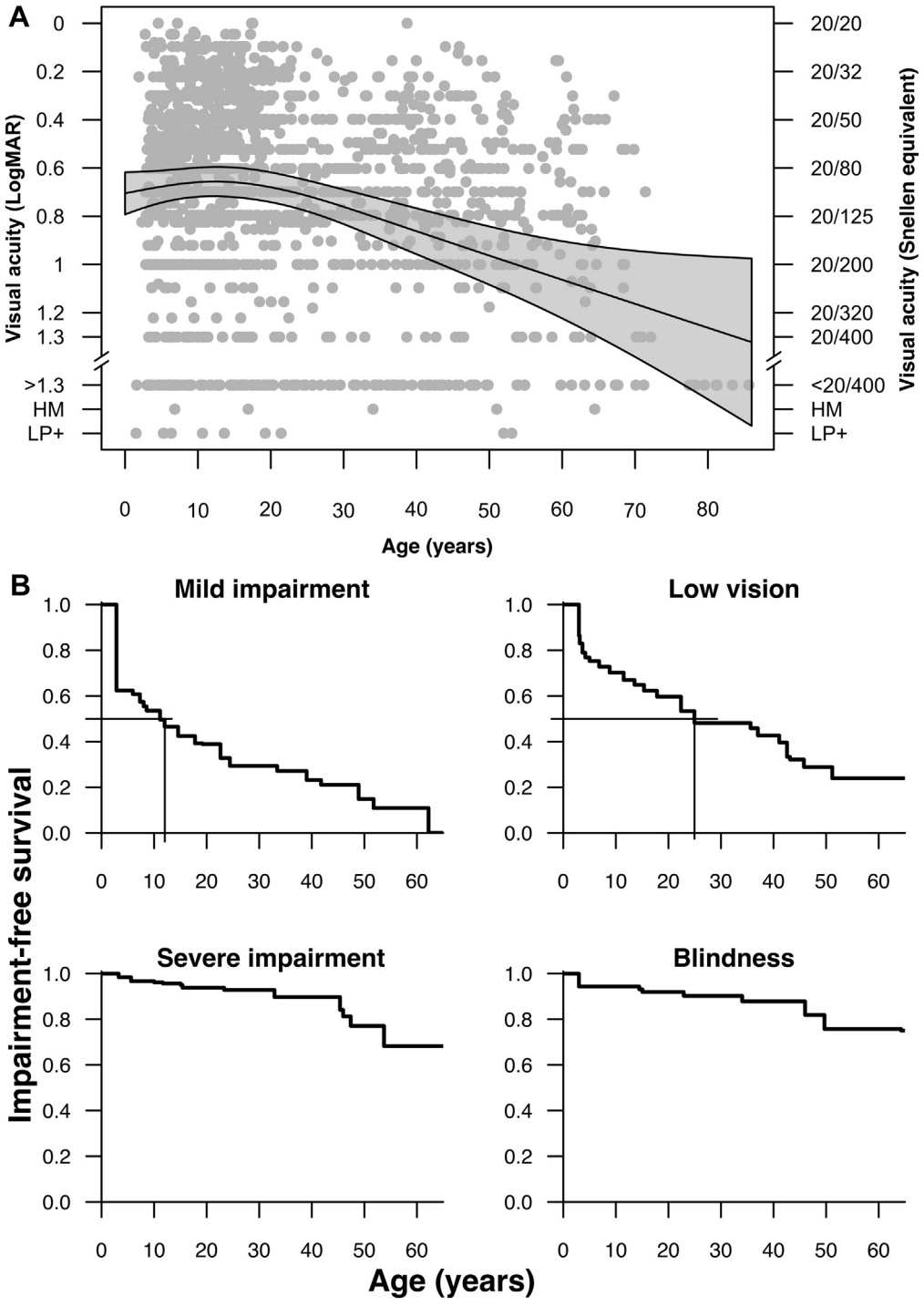

Figure 1. Graphs showing the evolution of visual acuity (VA) and visual impairment with advancing age in patients with X-linked retinoschisis. **A**, Linear mixed-effects model using VA measurements of the right eye to predict the average evolution of VA with increasing age. The mean VA increased slightly in the first 2 decades of life and then transitioned to a relatively constant slow decline. Over the entire population, a significant annual decline of 0.44% per year ($P < 0.001$) was found. **B**, Survival curves illustrating the time to reach mild impairment (20/40 > VA ≥ 20/70), low vision (20/70 > VA ≥ 20/200), severe visual impairment (20/200 > VA ≥ 20/400), and blindness (VA, < 20/400) in the right eye (as defined by the World Health Organization). To account for censored data, a nonparametric likelihood estimator was used. HM = hand movements; logMAR = logarithm of the minimum angle of resolution; LP+ = light perception.

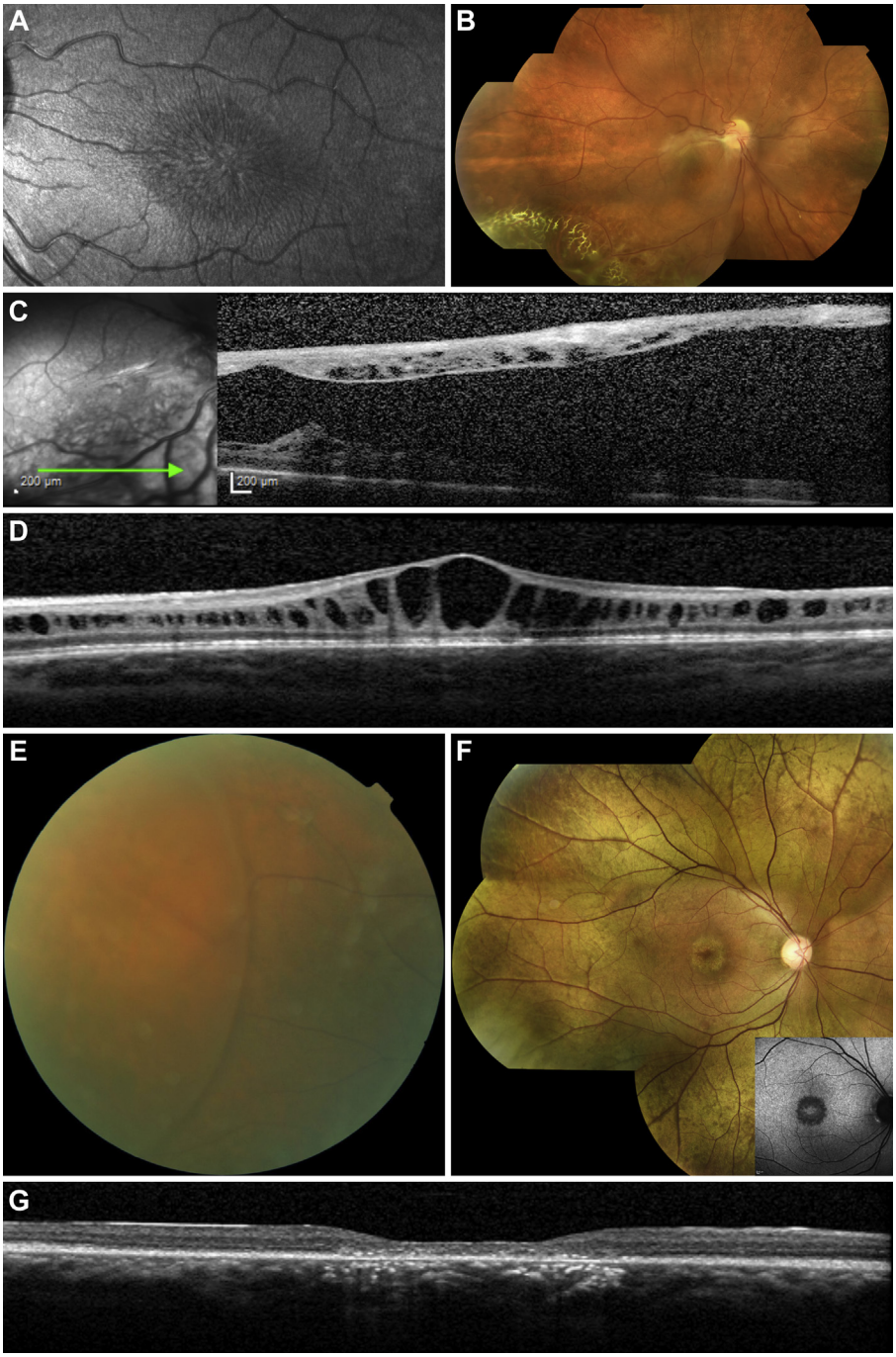

Figure 2. Typical findings in patients with X-linked retinoschisis (XLRS). **A**, Infrared fundus photography of a 4-year-old patient showing a macular spoke-wheel pattern. This patient carried a c.422G→A (p.Arg141His) variant in the *RS1* gene (visual acuity [VA] in the right eye, 20/60; VA in the left eye, 20/200; amblyopia in left eye resulting from anisometropia). **B**, **C**, Fundus photograph of the right eye of an 18-year-old patient (c.214G→A (p.Glu72Lys) variant in *RS1* gene) (**B**) and spectral-domain (SD) OCT image (**C**) acquired at 15 years of age. Lattice-like lesions and peripheral schisis are present inferotemporally, as displayed on the SD OCT. Also, an epiretinal membrane of the macula is present. This patient also had a Coats-like peripheral vascular lesion with hard exudates in the right eye at 14 years of age that resolved spontaneously. The VA in this eye was 20/400. **D**, SD OCT image showing typical macular schisis features in a 10-year-old patient with XLRS (c.598C→T (p.Arg200Cys) variant in *RS1*). The VA was 20/60 in both eyes. **E**, Fundus photograph of the right eye of a 56-year-old patient with XLRS (c.214G→A (p.Glu72Lys) *RS1* variant) showing extensive inferotemporal bullous peripheral schisis. **F**, Color fundus photograph from a 44-year-old patient with XLRS (c.566del p.(Leu189Argfs*48) variant in the *RS1* gene) showing macular atrophic changes and a so-called golden sheen of the fundus outside the macula. The fundus autofluorescence image in the lower right corner inset shows a hypoautofluorescent ring surrounding the fovea corresponding to atrophy of the retinal pigment epithelium. **G**, Central foveal SD OCT scan of a patient showing macular atrophy and discontinuous photoreceptor layers, especially in the perifoveal area. The VA was 20/125 in the right and 20/55 in the left eye.

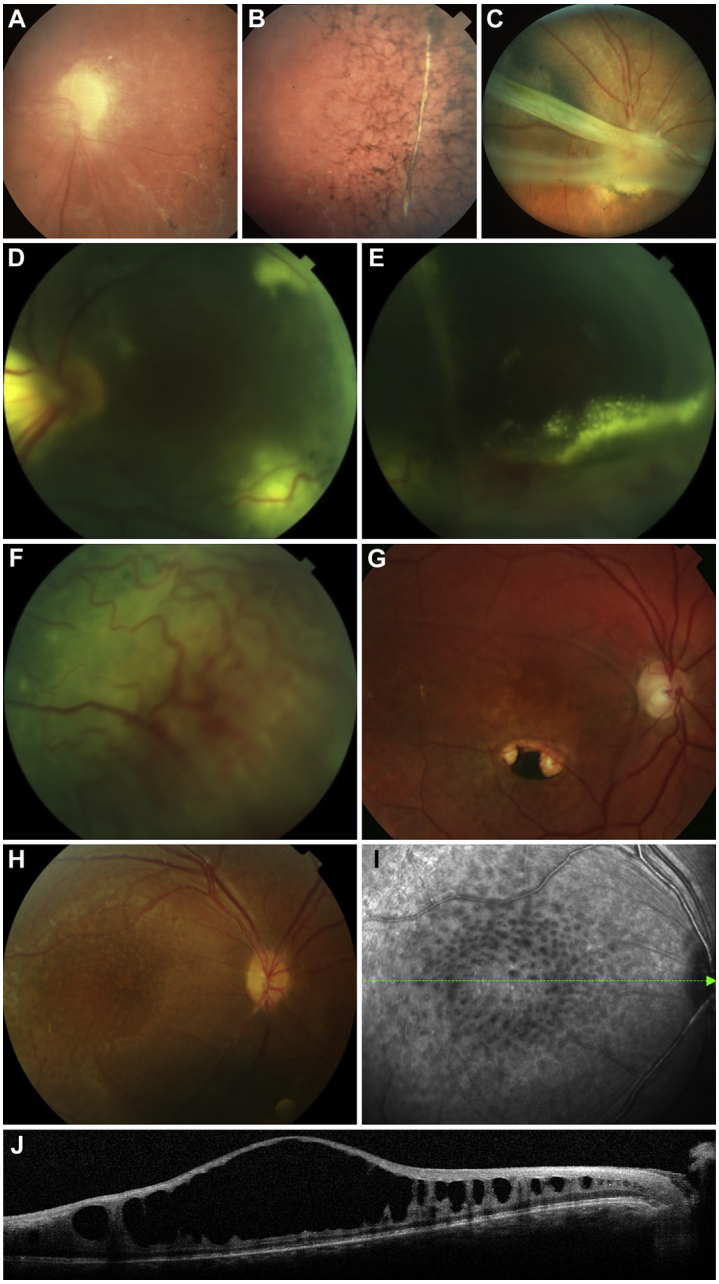

Figure 3. Fundus photographs and a spectral-domain (SD) OCT image showing relatively atypical retinal abnormalities in X-linked retinoschisis (XLRS). **A**, **B**, Right eye of a 22-year-old patient with optic disc pallor, a retinitis pigmentosa-like aspect, and a retinal fold in the temporal retina. This eye sustained a retinal detachment when the patient was 4 years of age that resulted in permanent decline in visual acuity (VA) to light perception. This previous retinal detachment may have been responsible for the aforementioned fundus changes. The left eye displayed a spoke-wheel pattern and a VA of 20/50. A c.436G→A (p.Glu146Lys) variant in the *RS1* gene was confirmed. **C,** Fundus photograph from a 14-year-old patient with XLRS showing a horizontal falciform retinal fold reaching from the optic disc to the temporal periphery in the right eye. The fold is crossing the macular area, which was displaced superiorly. The VA was 20/300 in the right eye and 20/600 in the left eye. The left eye showed extensive schisis including the macula, but no explanation for the low VA was found in the medical record or on imaging. **D**–**F**, Left eye of a patient (c.214G→A (p.Glu72Lys) variant in *RS1*) with Coats-like vascular anomalies, leakage of hard exudates, and an exudative retinal detachment sustained at 22 years of age. The eye was treated with injections of intravitreal bevacizumab and laser coagulation to prevent atrophy of the globe. One year later, rubeosis of the iris and slight phthisis in this eye developed that were managed successfully with repeated peripheral iridectomy and brinzolamide. The treatments were successful in preventing progressive phthisis, but VA remained poor (20/600). Because of familial predisposition for glaucoma and narrow chamber angles, the right eyeunderwent a preventive peripheral iridectomy as well. The right eye showed typical signs of XLRS described as macular spoke-wheel pattern and a golden sheen with lattice-like lesions in the peripheral retina. The VA was 20/125 in the right eye. **G**, Fundus photograph from a 10-year-old patient with a deletion of exon 3 (c.78+365_184+607del (p.?) in the *RS1* gene) showing a chorioretinal scar in the inferior macula in the right eye. The scar, resembling a toxoplasma-like scar or a torpedo maculopathy-like lesion, was described first at 1 year of age. The VA was 20/600 in this eye and 20/60 in the left eye, which showed typical XLRS changes in the macula, without such a scar. **H**, **I**, Fundus photograph (**H**) and infrared photographs (**I**) showing fundus albipunctatus-like yellow-white deposits in the right eye of an 8-year-old patient (c.577C→T (p.Pr0193Ser) variant in the *RS1* gene). **J**, SD OCT image of this patient showing extensive central schisis with large cysts present in the macula. The left eye was amblyopic. The VA was 0.125 in the right and 20/200 in the left eye.

(38 patients [14.6%]), and c.598C→T (p.(Arg200Cys); 11 patients [4.2%]; Table S4, available at www.aaojournal.org). In total, 158 of 261 patients (60.5%) were classified as having variants that were predicted to be mild (missense variant), and 103 of 261 patients (39.5%) were classified as having severe variants (deletions, nonsense, splice site, frameshift, and cysteine substitution-causing variants).

Discussion

In this large follow-up study of XLRS, data from 340 patients from 8 different centers in 2 different Northern European countries were included. We examined the phenotypic spectrum, long-term natural history, and genotype. In general, the funduscopic findings were similar compared with those reported in earlier literature.[5,7] Macular changes were the most commonly described ophthalmoscopic findings, with foveal schisis in 70.4% of patients. Macular abnormalities were described as a spoke-wheel pattern in only in 50.7% of patients. Slightly more than half of the patients had peripheral retinoschisis, which is roughly comparable with that reported in earlier studies.[4,5] Interestingly, optic disc pallor was reported in 15.8% of patients in this cohort, which was been found in a smaller study of 22 patients in combination with retinal nerve fiber layer thinning on SD OCT.[27] In a 3-dimensional retinal organoid model of XLRS derived from a patient with the c.625C→T (p.Arg209Cys) variant in the *RS1* gene, progressive loss of *OPA1* gene expression was described.[28] *OPA1* encodes the mitochondrial dynamin-like GTPase protein that normally localizes to the inner mitochondrial membrane, where it plays an important role in mitochondria-associated cellular processes. Mutations in *OPA1* are the most common cause of autosomal dominant optic atrophy, making it plausible that decreased *OPA1* expression in XLRS may contribute to the development of ganglion cell dysfunction and optic disc pallor in some patients with XLRS. Besides this potential role of decreased *OPA1* expression on retinal (ganglion) cellular dysfunction and optic disc pallor in XLRS, a primary effect of the retinoschisis maculopathy on the development of optic disc pallor also may be a factor.

Most patients with XLRS in the current study demonstrated mild to moderate visual impairment with a median VA of 0.60 logMAR (Snellen equivalent, 20/80) in the right eye and 0.53 logMAR (Snellen equivalent, 20/68) in the left eye at a mean age of 28.6 years, which is similar to that reported in earlier studies.[6,7,29,30] Interestingly, a recent Chinese study reported a remarkably low mean VA of 0.81 logMAR (Snellen equivalent, 20/129) in a cohort of 90 patients at a mean age of just 17.29 ± 12.94 years, which indicates that XLRS may be more severe in some populations.[31] Linear mixed-model analysis using the VA of the right eye predicted a slow but significant annual VA decline of 0.44%, which is comparable with the slow decline described in earlier cross-sectional and longitudinal cohorts.[6,7,29–31] In the current study, predominantly patients older than 40 years started to demonstrate severe visual impairment and blindness, which occurred in approximately 35% and 25% of patients at the age of 60 years, respectively. This is comparable with earlier studies, in which severe visual impairment of worse than 20/200 Snellen equivalent was described in 38% to 58% of patients older than 40 years, but it was not always specified whether the VA of one eye, the better-seeing eye, or both eyes was used.[5,8] Analyzing both eyes combined, or the better-seeing eye, without taking the between-eye correlation into account, may result in a bias of the reported VA and severity of visual impairment in XLRS. This may explain, in part, the differences between studies and should be taken into consideration in future studies.[26] A prospective study reported a comparably high VA of approximately 0.46 logMAR (Snellen equivalent, 20/58) in the right and left eye at a mean age of 30.0 years, but this finding may be explained, at least in part, by the fact that patients with vision-threatening complications such as retinal detachment were excluded from the study.[5] Noteworthy in our study is that the VA in this cohort initially seemed to increase slightly within the first 2 decades of life and transitioned into a slow decrease starting approximately from the age of 12 years (Fig 1). The initial increase of VA at a young age may be the result of multiple factors, such as inadequate reliability of measuring VA in young children, maturation of the visual system, or both. This potential trend should be researched further and considered when evaluating development of VA in future natural history and therapeutic studies for XLRS or possibly even other juvenile ocular diseases. Previously, mostly linear analyses of VA evolution have been used, but splines or other non-linear methods may facilitate a more accurate representation of the evolution of continuous measures in some large cohorts. In general, the evolution of VA found in this study is in accordance with that found in previous studies, which describe an accelerated decline of VA resulting from the development of atrophy of the neuroretina and RPE, which becomes more pronounced around 30 years of age.[1,7,32] Our study suggests that this transition is generally a slow and gradual process, but may differ in speed and severity in each individual. A large variability in phenotype as well as natural course within each age group, family, and genotype, and even between eyes of individual patients with XLRS, was seen in this and earlier cohorts.[1,5–7]

A wide range of different disease-causing variants in the *RS1* gene have been found in the current study, with most variants being missense variants and a smaller percentage of deletions, nonsense variants, and splice-site variants. Most of these variants were found in the discoidin domain located in exons 4 to 6. Similar distributions and location of variants have been described in earlier large studies.[5–7,14] Remarkably, the c.214G→A p.(Glu72Lys) was found in nearly 40% of all patients with XLRS in this cohort. The same variant has been described commonly in different European and international cohorts as one of the most prevalent variants. It was found in 76 out of 108 Finnish patients (70.4%), in 5 of 25 Hungarian patients (20.0%), in 16 of 86 patients (18.6%) from the United Kingdom, in 3 of 18 Italian patients (16.6%), in 5 of 34 Spanish families (14.7%), in 7 of 56 Japanese families (12.5%), in 5 of 56

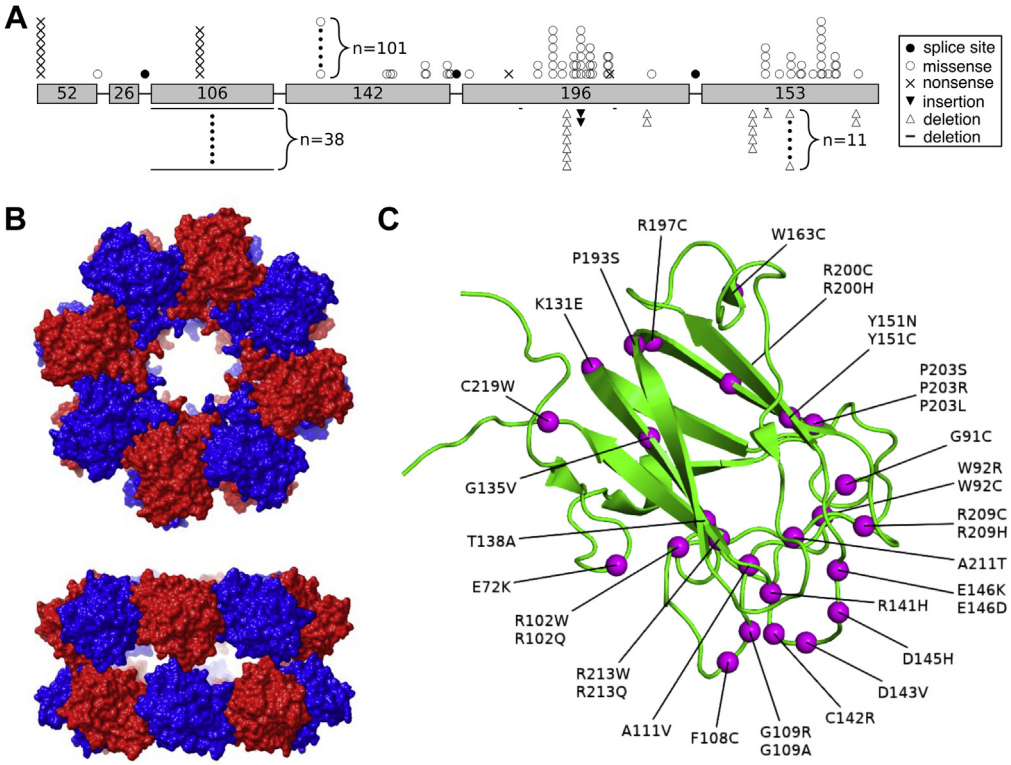

Figure 4. Locations of variants found in this study, displayed schematically in the *RS1* gene and retinoschisin protein. **A**, Schematic drawing of the *RS1* gene with the 6 exons represented by boxes and their length indicated by the number of containing nucleotides. Introns are drawn as connecting lines between the exons. The variants are marked by the symbols illustrated in the legend (one for each patient found with that variant). The frequencies of the 3 most common variants are written next to the corresponding symbols. **B**, Top and side view of a retinoschisin double octamer containing 16 subunits marked in red and blue. **C**, Locations of found missense variants in a 3-dimensional model of a mature retinoschisin subunit. Variants are indicated as pink spheres. The *RS1* domain and C-terminal are not illustrated because the structure is not known yet.

patients (8.9%) from the United States, and in 4 of 90 in Chinese patients (4.4%), but in only 1 of 52 French patients (1.9%) and in none of 21 Australian patients.[5–7,29–31,33–36] This may indicate that the c.214G→A p.(Glu72Lys) may be one of the most common variants causing XLRS worldwide and is especially prevalent in the Dutch and Belgian populations. The second most common variant in the current study was a deletion of exon 3 in 38 of 261 patients (14.6%) and was described in only 1 of 56 Japanese families (1.7%) from among the aforementioned studies.[30] However, other large deletions involving one or multiple exons have been described regularly in multiple XLRS studies.[5,7,30,31] The relatively high prevalence of these variants in the Dutch and Belgian patients in this study may be caused by a founder effect. However, it has also been hypothesized that the high prevalence of certain common XLRS variants, such as the one described above, not only may be caused by a founder effect, but also by mutation hot spots in the *RS1* gene.[14] Despite the large amount of clinical long-term follow-up data and broad range of *RS1* variants, we did not find a clear genotype–phenotype correlation for VA, which is in line with earlier findings.[6,29,31] However, studies by Bowles et al[23] and Vincent et al[15] suggest that b-wave amplitude and the b-to-a amplitude ratio are significantly lower in patients with variants that are genetically severe compared with those with mild variants, whereas other literature studies report that determining a clear genotype–phenotype correlation using electroretinography may be difficult.[5,30] The current study had mainly categorical electroretinography data available, and therefore could not replicate these analyses.

Nearly all patients in this study displayed a reduced b-to-a amplitude ratio on electroretinography, with an additional electronegative aspect of the combined rod-cone response to a high-intensity flash in the dark-adapted patient in 72.2%, which is consistent with previous findings.[5,7,23] The electroretinography findings were normal in 2 patients (3 and 6 years of age) with a typical XLRS phenotype and a confirmed *RS1* variant, which demonstrates that normal electroretinography findings at young age may not exclude the diagnosis of XLRS. On SD OCT, macular schisis and atrophy were found more frequently as compared with ophthalmoscopy, indicating that SD OCT is crucial for diagnosis, staging, and follow-up of XLRS. Central retinal thickness did not correlate with VA in this study, as described previously in a smaller study.[5] However, in our study, a decrease in foveal PROS length and a compromised integrity of ELM, as well as the EZ layer, correlated significantly with age and decreased VA, which is similar to the findings of Ores et al.[7] Interestingly, *Rs1* knockout mouse models have shown a similar natural course on histologic analysis, with an increase in schisis cavities until the fourth month after birth, after which the

cavities disappeared over a span of 8 months, with a slowly progressive photoreceptor degeneration with increasing age.[37] Gene therapy in these mice at 7 months after birth did not result in any improvement on electroretinography as compared with that seen in mice treated before 2 months after birth, although significant photoreceptor preservation on histologic analysis remained when comparing treated and untreated eyes.[38]

The findings that gene therapy in mice seemed to slow down photoreceptor degeneration, in combination with the relatively slow visual decline during follow-up in human studies, may imply that the window of opportunity for intervention in XLRS could be relatively large in terms of rescue of (photoreceptor) cellular function. Selecting patients at an age before significant vision loss resulting from photoreceptor degeneration may optimize the treatment effect and likelihood of cell rescue and preservation of VA. Bearing this in mind, the natural course presented in this study suggests that the optimal window for intervention may be within the first 2 to 3 decades of life, before the progression of XLRS generally seems to accelerate due to the development of retinal atrophy. However, given the large phenotypic variability, photoreceptor integrity on SD OCT may be a better tool to select optimal candidates for future interventional trials. An *Rs1* knockout mouse model by Gehrig et al[39] demonstrated a peak apoptotic activity in photoreceptors in mice as early as 18 days after birth, which may indicate that some photoreceptor loss may have already occurred shortly after birth. No human studies to date have described the phenotype and course of XLRS shortly after birth, because symptoms are generally noted only from preschool age onward, and examination of visual function and retinal structure in infants can be challenging. The use of handheld SD OCT may reveal more details about the early human natural course of XLRS in the future. In the current cohort, we found a subset of 24 patients who received a diagnosis at 40 years of age or older and had relatively mild, late-onset visual symptoms and an atypical phenotype led to a challenging and delayed diagnosis of XLRS. These patients generally did not show any schisis, but only mild to moderate photoreceptor and RPE atrophy on SD OCT (Fig 2G). On opthalmoscopy, modest atrophic RPE changes, a metallic sheen in the macula, or both were described (Fig 2F). In 2 of these patients (0.8%), the phenotype was recognized as an atypical late-onset presentation of XLRS only after a pathogenic *RS1* variant in the patients was found with genetic analysis or after a younger affected family member was diagnosed with a typical XLRS phenotype, leading to DNA testing.

The current study is subject to the known limitations of retrospective clinical data from medical records, such as missing data, unstandardized examinations of VA, irregularities in follow-up intervals, and limited availability of longitudinal electroretinography examinations, OCT scans, or fundus autofluorescence images. Despite VA not being obtained by a standard protocol, the data were reviewed carefully for outliers, and with a total of approximately 1940 VA data points for each eye, we believe that this dataset enables a relatively accurate and unique evaluation of long-term visual function in XLRS. Large, prospective natural history studies, including extensive structural and functional parameters, will provide the most reliable and standardized information on the disease course of hereditary retinal diseases.[5] However, although long-term follow-up may be needed in many of these diseases to allow for the identification of optimal disease-specific clinical outcome measures, the extent and duration of such studies are associated with high costs and logistic challenges.[5,40,41] Therefore, retrospective studies, such as the present study, can offer vast amounts of data from a large cohort with a long follow-up time, including phenotypic and functional development.

In summary, this multicenter study found a large variability in visual function and clinical course in patients with XLRS, in association with a broad range of *RS1* variants. No clear genotype−phenotype correlation was identified. In the great majority of patients with XLRS, the VA remained relatively stable or possibly even increased in the first 2 decades of life, suggesting that the optimal window of opportunity for treatment may be within the first 2 to 3 decades of life. However, VA can be relatively preserved in the ensuing decades and showed only a slow decline, indicating that a broader therapeutic intervention window may exist for XLRS, in which significant structural and functional rescue may still be achieved. Conversely, the slowly progressive nature of XLRS may complicate the identification of clinical end points to evaluate treatment success. Given the variability in phenotype, the integrity of EZ and ELM, and PROS length, on SD OCT may be useful structural parameters to guide the selection of suitable candidates for future (gene) therapeutic trials and may also be suitable as structural end points. However, to validate these structure−function correlations further, additional studies should be conducted, including repeatability assessment, longitudinal evaluation of imaging, and possibly prospective data. The elaborate clinical and genetic description of XLRS in this large cohort can be useful for clinicians during the diagnostic process and clinical counseling. Future research may also benefit from the presented data when choosing an appropriate study design for future treatment options.

Footnotes and Disclosures

Originally received: May 7, 2021.
Final revision: September 28, 2021.
Accepted: September 29, 2021.
Available online: October 6, 2021. Manuscript no. D-21-00937.

[1] Department of Ophthalmology, Amsterdam University Medical Centers, University of Amsterdam, Amsterdam, The Netherlands.

[2] Bartiméus, Diagnostic Center for Complex Visual Disorders, Zeist, The Netherlands.

[3] Department of Clinical Genetics, Amsterdam University Medical Centers, University of Amsterdam, Amsterdam, The Netherlands.

[4] Department of Epidemiology and Biostatistics, Amsterdam University Medical Centers, Amsterdam, The Netherlands.

[5] Department of Ophthalmology, University Hospital Ghent, Ghent University & Ghent University, Ghent, Belgium.

[6] Department of Ophthalmology, Erasmus Medical Center, Rotterdam, The Netherlands.

[7] Center for Medical Genetics Ghent, Ghent University Hospital & Ghent University, Ghent, Belgium.

[8] Department of Ophthalmology, Radboud University Medical Center, Nijmegen, The Netherlands.

[9] Institute of Molecular and Clinical Ophthalmology, University Hospital Basel, University of Basel, Basel, Switzerland.

[10] Department of Ophthalmology, University Medical Center Utrecht, Utrecht, The Netherlands.

[11] The Rotterdam Eye Hospital and the Rotterdam Ophthalmic Institute, Rotterdam, The Netherlands.

[12] Department of Ophthalmology, School of Medicine, University of California at Davis, Sacramento, California.

[13] Division of Ophthalmology & CCMT, The Children's Hospital of Philadelphia, Philadelphia, Pennsylvania.

[14] The Netherlands Institute for Neuroscience (NIN-KNAW), Royal Netherlands Academy of Arts and Sciences, Amsterdam, The Netherlands.

[15] Department of Ophthalmology, Leiden University Medical Center, Leiden, The Netherlands.

Presented at: Association for Research in Vision and Ophthalmology Annual Meeting, Virtual Congress, May 2021; European Society of Retina Specialists Annual Meeting, Virtual Congress, October 2020; and the International Society for Genetic Eye Diseases and Retinoblastoma Annual Meeting, Giessen, Germany, August 2019.

Disclosure(s):

All authors have completed and submitted the ICMJE disclosures form.

The author(s) have made the following disclosure(s):

C.C.W.K.: Consultant − Bayer, Thea Pharma

This research was supported by the ODAS Foundation (grant no: 2018-2) and the European Society of Retina Specialists (EURETINA Clinical Research Award 2019, grant no: 2019-1974 [L.C.H., C.J.F.B.]); the Ghent University Special Research Fund (grant nos.: BOF15/GOA/011 [E.D.B.] and BOF20/GOA/023 [E.D.B. and B.P.L.]); Ghent University Hospital Innovation Fund (grant NucleUZ [E.D.B.]); and Research Foundation - Flanders (senior clinical investigator grant nos.: 1802220N [E.D.B.] and 1803821N [B.P.L.]). The RD5000 consortium was supported by Uitzicht (grant 2015-30 financed by ODAS, Oogfonds, Retinafonds, and Bartiméus Sonneheerdt [C.C.W.K.]). The sponsors or funding organizations had no role in the design or conduct of this research. This study was performed as part of a collaboration within the European Reference Network for Rare Eye Diseases, of which E.D.B., C.C.W.K., L.I.v.d.B., C.B.H, B.P.L., A.A.B., and C.J.F.B. are members and which is co-funded by the Health Program of the European Union (Framework Partnership Agreement no.: 739534 'ERN-EYE').

HUMAN SUBJECTS: Human subjects were included in this study, but only retrospective data from medical records were used. The ethics committees at Amsterdam University Medical Centers and the Erasmus Medical Center approved this study. All research adhered to the tenets of the Declaration of Helsinki. Participants or their legal guardians provided informed consent. The need for informed consent was waived by the local ethics committee of the University Hospital Ghent because of the use of retrospective pseudonymized data.

No animal subjects were included in this study.

Author Contributions:

Conception and design: Hahn, van Schooneveld, Wesseling, Lissenberg-Witte, Leroy, Bergen, Boon

Analysis and interpretation: Hahn, van Schooneveld, Florijn, Lissenberg-Witte, Meester-Smoor, Diederen, Klaver, Ossewaarde-van Norel, van den Born, Hoyng, van Genderen, Sieving, Leroy, Bergen, Boon

Data collection: Hahn, Wesseling, ten Brink, Strubbe, Meester-Smoor, Thiadens, Diederen, van Cauwenbergh, de Zaeytijd, Walraedt, de Baere, Klaver, Ossewaarde-van Norel, van den Born, Hoyng, van Genderen, Sieving, Leroy, Bergen, Boon

Obtained funding: Study was performed as part of the authors' regular employment duties. No additional funding was provided.'

Overall responsibility: Hahn, van Schooneveld, Wesseling, Florijn, ten Brink, Lissenberg-Witte, Strubbe, Meester-Smoor, Thiadens, Diederen, van Cauwenbergh, de Zaeytijd, Walraedt, de Baere, Klaver, Ossewaarde-van Norel, van den Born, Hoyng, van Genderen, Sieving, Leroy, Bergen, Boon

Abbreviations and Acronyms:
D = diopter; **ELM** = external limiting membrane; **EZ** = ellipsoid zone; **IQR** = interquartile range; **logMAR** = logarithm of the minimum angle of resolution; **PROS** = photoreceptor outer segment; **RPE** = retinal pigment epithelium; **SD** = spectral-domain; **VA** = visual acuity; **XLRS** = X-linked retinoschisis.

Keywords:
Genotype, Natural history, Phenotype, Surrogate end points, X-linked retinoschisis.

Correspondence to:
Camiel J. F. Boon, MD, PhD, Department of Ophthalmology, Amsterdam Medical Center, P. O. Box 22660, 1100 DD Amsterdam, The Netherlands. E-mail: Camiel.boon@amsterdamumc.nl.

References

1. Molday RS, Kellner U, Weber BH. X-linked juvenile retinoschisis: clinical diagnosis, genetic analysis, and molecular mechanisms. *Prog Retin Eye Res*. 2012;31(3):195−212.
2. Haas J. Ueber das Zusammenvorkommen von Veraenderungen der Retina und Choroidea. *Arch Augenheilkd*. 1898;37:343−348.
3. Jager GM. A hereditary retinal disease. *Trans Ophthalmol Soc UK*. 1953;73:617−619.
4. George ND, Yates JR, Bradshaw K, Moore AT. Infantile presentation of X linked retinoschisis. *Br J Ophthalmol*. 1995;79(7):653−657.
5. Pennesi ME, Birch DG, Jayasundera KT, et al. Prospective evaluation of patients with X-linked retinoschisis during 18 months. *Invest Ophthalmol Vis Sci*. 2018;59(15):5941−5956.
6. Pimenides D, George NDL, Yates JRW, et al. X-linked retinoschisis: clinical phenotype and RS1 genotype in 86 UK patients. *J Med Genet*. 2005;42(6):e35.
7. Ores R, Mohand-Said S, Dhaenens CM, et al. Phenotypic characteristics of a French cohort of patients with X-linked retinoschisis. *Ophthalmology*. 2018;125(10):1587−1596.
8. Apushkin MA, Fishman GA, Rajagopalan AS. Fundus findings and longitudinal study of visual acuity loss in patients with X-linked retinoschisis. *Retina*. 2005;25(5):612−618.
9. Kim LS, Seiple W, Fishman GA, Szlyk JP. Multifocal ERG findings in carriers of X-linked retinoschisis. *Doc Ophthalmol*. 2007;114(1):21−26.

10. Sikkink SK, Biswas S, Parry NR, et al. X-linked retinoschisis: an update. *J Med Genet*. 2007;44(4):225–232.
11. Rodriguez FJ, Rodriguez A, Mendoza-Londono R, et al. X-linked retinoschisis in three females from the same family: a phenotype-genotype correlation. *Retina*. 2005;25(1):69–74.
12. Ou J, Vijayasarathy C, Ziccardi L, et al. Synaptic pathology and therapeutic repair in adult retinoschisis mouse by AAV-RS1 transfer. *J Clin Invest*. 2015;125(7):2891–2903.
13. Tolun G, Vijayasarathy C, Huang R, et al. Paired octamer rings of retinoschisin suggest a junctional model for cell–cell adhesion in the retina. *Proc Natl Acad Sci U S A*. 2016;113(19):5287.
14. The Retinoschisis Consortium. Functional implications of the spectrum of mutations found in 234 cases with X-linked juvenile retinoschisis. *Hum Mol Genet*. 1998;7(7):1185–1192.
15. Vincent A, Robson AG, Neveu MM, et al. A phenotype-genotype correlation study of X-linked retinoschisis. *Ophthalmology*. 2013;120(7):1454–1464.
16. Kim DY, Mukai S. X-linked juvenile retinoschisis (XLRS): a review of genotype-phenotype relationships. *Semin Ophthalmol*. 2013;28(5–6):392–396.
17. Verbakel SK, van de Ven JP, Le Blanc LM, et al. Carbonic anhydrase inhibitors for the treatment of cystic macular lesions in children with X-linked juvenile retinoschisis. *Invest Ophthalmol Vis Sci*. 2016;57(13):5143–5147.
18. Apushkin MA, Fishman GA. Use of dorzolamide for patients with X-linked retinoschisis. *Retina*. 2006;26(7):741–745.
19. Bush RA, Zeng Y, Colosi P, et al. Preclinical dose-escalation study of intravitreal AAV-RS1 gene therapy in a mouse model of X-linked retinoschisis: dose-dependent expression and improved retinal structure and function. *Hum Gene Ther*. 2016;27(5):376–389.
20. Ye GJ, Conlon T, Erger K, et al. Safety and biodistribution evaluation of rAAV2tYF-CB-hRS1, a recombinant adeno-associated virus vector expressing retinoschisin, in RS1-deficient mice. *Hum Gene Ther Clin Dev*. 2015;26(3):177–184.
21. Turriff A, Blain D, Similuk M, et al. Motivations and decision making processes of men with X-linked retinoschisis considering participation in an ocular gene therapy trial. *Am J Ophthalmol*. 2019;204:90–96.
22. van Huet RA, Oomen CJ, Plomp AS, et al. The RD5000 database: facilitating clinical, genetic, and therapeutic studies on inherited retinal diseases. *Invest Ophthalmol Vis Sci*. 2014;55(11):7355–7360.
23. Bowles K, Cukras C, Turriff A, et al. X-linked retinoschisis: RS1 mutation severity and age affect the ERG phenotype in a cohort of 68 affected male subjects. *Invest Ophthalmol Vis Sci*. 2011;52(12):9250–9256.
24. Almoqbel FM, Irving EL, Leat SJ. Visual acuity and contrast sensitivity development in children: sweep visually evoked potential and psychophysics. *Optom Vis Sci*. 2017;94(8):830–837.
25. Leat SJ, Yadav NK, Irving EL. Development of visual acuity and contrast sensitivity in children. *J Optom*. 2009;2(1):19–26.
26. Armstrong RA. Statistical guidelines for the analysis of data obtained from one or both eyes. *Ophthalmic Physiol Opt*. 2013;33(1):7–14.
27. Genead MA, Pasadhika S, Fishman GA. Retinal nerve fibre layer thickness analysis in X-linked retinoschisis using Fourier-domain OCT. *Eye*. 2009;23(5):1019–1027.
28. Huang KC, Wang ML, Chen SJ, et al. Morphological and molecular defects in human three-dimensional retinal organoid model of X-linked juvenile retinoschisis. *Stem Cell Rep*. 2019;13(5):906–923.
29. Riveiro-Alvarez R, Trujillo-Tiebas M-J, Gimenez-Pardo A, et al. Correlation of genetic and clinical findings in Spanish patients with X-linked juvenile retinoschisis. *Invest Ophthalmol Vis Sci*. 2009;50(9):4342–4350.
30. Kondo H, Oku K, Katagiri S, et al. Novel mutations in the RS1 gene in Japanese patients with X-linked congenital retinoschisis. *Hum Genome Var*. 2019;6:3.
31. Chen C, Xie Y, Sun T, et al. Clinical findings and RS1 genotype in 90 Chinese families with X-linked retinoschisis. *Mol Vis*. 2020;26:291–298.
32. Wood EH, Lertjirachai I, Ghiam BK, et al. The natural history of congenital X-linked retinoschisis and conversion between phenotypes over time. *Ophthalmol Retina*. 2019;3(1):77–82.
33. Lesch B, Szabó V, Kánya M, et al. Clinical and genetic findings in Hungarian patients with X-linked juvenile retinoschisis. *Mol Vis*. 2008;14:2321–2332.
34. Simonelli F, Cennamo G, Ziviello C, et al. Clinical features of X linked juvenile retinoschisis associated with new mutations in the XLRS1 gene in Italian families. *Br J Ophthalmol*. 2003;87(9):1130–1134.
35. Hewitt AW, FitzGerald LM, Scotter LW, et al. Genotypic and phenotypic spectrum of X-linked retinoschisis in Australia. *Clin Exp Ophthalmol*. 2005;33(3):233–239.
36. Huopaniemi L, Rantala A, Forsius H, et al. Three widespread founder mutations contribute to high incidence of X-linked juvenile retinoschisis in Finland. *Eur J Hum Genet*. 1999;7(3):368–376.
37. Kjellstrom S, Bush RA, Zeng Y, et al. Retinoschisin gene therapy and natural history in the Rs1h-KO mouse: long-term rescue from retinal degeneration. *Invest Ophthalmol Vis Sci*. 2007;48(8):3837–3845.
38. Janssen A, Min SH, Molday LL, et al. Effect of late-stage therapy on disease progression in AAV-mediated rescue of photoreceptor cells in the retinoschisin-deficient mouse. *Mol Ther*. 2008;16(6):1010–1017.
39. Gehrig A, Janssen A, Horling F, et al. The role of caspases in photoreceptor cell death of the retinoschisin-deficient mouse. *Cytogenet Genome Res*. 2006;115(1):35–44.
40. Thompson DA, Iannaccone A, Ali RR, et al. Advancing clinical trials for inherited retinal diseases: recommendations from the Second Monaciano Symposium. *Transl Vis Sci Technol*. 2020;9(7), 2–2.
41. Talib M, Boon CJF. Retinal dystrophies and the road to treatment: clinical requirements and considerations. *Asia Pac J Ophthalmol (Phila)*. 2020;9(3):159–179.